

# ROAD-Waymo: Action Awareness at Scale for Autonomous Driving

Salman Khan<sup>1</sup>, Izzeddin Teeti<sup>1</sup>, Reza Javanmard Alitappeh<sup>2</sup>, Mihaela C. Stoian<sup>3</sup>, Eleonora Giunchiglia<sup>4</sup>, Gurkirt Singh<sup>5</sup>, Andrew Bradley<sup>1</sup>, and Fabio Cuzzolin<sup>1</sup>

<sup>1</sup> Oxford Brookes University, United Kingdom

<sup>2</sup> MAZUST, Iran

<sup>3</sup> University of Oxford, United Kingdom

<sup>4</sup> Imperial College London, United Kingdom

<sup>5</sup> Xovis AG, Switzerland

**Abstract.** Autonomous Vehicle (AV) perception systems require more than simply seeing, via e.g., object detection or scene segmentation. They need a holistic understanding of what is happening within the scene for safe interaction with other road users. Few datasets exist for the purpose of developing and training algorithms to comprehend the actions of other road users. This paper presents ROAD-Waymo, an extensive dataset for the development and benchmarking of techniques for agent, action, location and event detection in road scenes, provided as a layer upon the (US) Waymo Open dataset. Considerably larger and more challenging than any existing dataset (and encompassing multiple cities), it comes with 198k annotated video frames, 54k agent tubes, 3.9M bounding boxes and a total of 12.4M labels. The integrity of the dataset has been confirmed and enhanced via a novel annotation pipeline designed for automatically identifying violations of requirements specifically designed for this dataset. As ROAD-Waymo is compatible with the original (UK) ROAD [57] dataset, it provides the opportunity to tackle domain adaptation between real-world road scenarios in different countries within a novel benchmark: ROAD++. Dataset and code are available at: Dataset <sup>6</sup>, Code <sup>7</sup>.

## 1 Introduction

Several large-scale, comprehensive AV training datasets have recently been released [9, 20, 45, 56, 65, 69], leveraging multiple sensors (*e.g.* cameras, LiDAR, GPS, *etc.*) for the purposes of object detection, semantic segmentation, object tracking and trajectory forecasting. However, a safe interaction with other road users requires much more than simply *seeing* things: rather, it requires understanding actions and events being conducted or happening in the scene. To this end, Singh *et al.* [57] introduced the ROAD dataset, which provides multi-label

<sup>6</sup> <https://github.com/salmank255/Road-waymo-dataset>

<sup>7</sup> [https://github.com/salmank255/ROAD\\_Waymo\\_Baseline](https://github.com/salmank255/ROAD_Waymo_Baseline)

annotations of agents and actions for event awareness in autonomous driving. ROAD represents a starting point along the path to enable AVs to understand events. It features some degree of diversity in terms of weather conditions (including bright sunshine, wet roads, rain, snow and fog) and can be used as a benchmark for object/agent detection, action detection and event detection in a natural multi-label setting. This was indeed the case for the ICCV 2021 ROAD workshop and challenge<sup>8</sup>, which saw a combined 200+ entries for the aforementioned tasks. Since then, the problem of situation awareness for AVs has gained even more traction [22, 70].

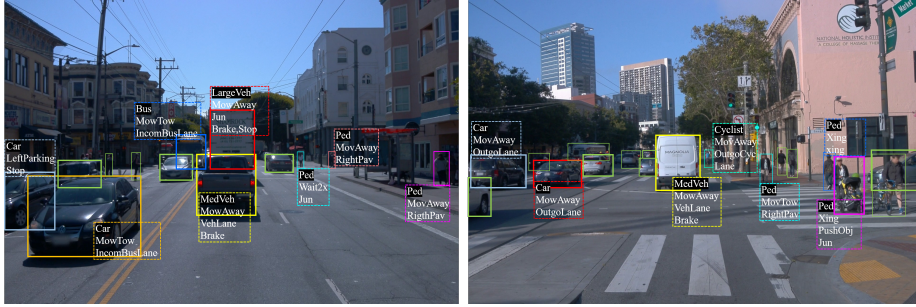


**Fig. 1:** Exemplary annotations of road users in ROAD-Waymo style, explained from the (ego) viewpoint of an AV. Each road user is annotated with three distinct labels: agent, action, and location. Only agents with a distinct status are labeled to avoid confusion from overlapped labels.

Nevertheless, ROAD remains a small-scale dataset, lacking in both scale and true diversity to allow the further demonstration and testing of the benefits of event awareness. It is limited to scenes from just one, relatively small city - Oxford, UK (population 160,000) - with a high density of narrow streets, relatively low-speed driving on few routes. This makes it suitable for early stage development, but is significantly less challenging than real-world driving in complex environments.

This paper introduces ROAD-Waymo, which tackles the diversity and scale issues of ROAD [57], building on the Waymo-Open dataset [61]. Spatiotemporal [57] annotations, in the form of agent tracks plus action and location labels, are densely provided in the scene to study event awareness, action and event detection. As such annotations are expensive - we inherited 52K tracks from the Waymo dataset, adding extensive labelling based upon the *road event* = { *agent*, *action*, *location* } protocol (illustrated in Figure 1), resulting in 4.1M bounding boxes with 4.1M agent, 4.3M action, and 4.3M location label instances.

In combination with the 7K tracks present in ROAD, ROAD-Waymo provides an extensive playground for the development of advanced perception systems for autonomous vehicles and the tackling of novel problems, with a focus

<sup>8</sup> <https://sites.google.com/view/roadchallengeiccv2021/challenge>



on domain adaption (in particular, between cities in the UK and the US) for action/agent/event detection tasks.

**Contributions:** The contributions of this work are:

1. **ROAD-Waymo** A large-scale multi-label dataset for action and event detection in autonomous vehicles. Provided as an extension to the Waymo AV dataset [61], it is considerably more comprehensive and challenging than any existing such benchmark, including ROAD.
2. **Scale:** ROAD-Waymo contains 4.3M action labels, making it 7 times larger than the original ROAD dataset, and the largest known dataset for this purpose. At the same time, it extends the Waymo dataset by providing a total of 12.7M additional labels.
3. **Multi-City:** The dataset encompasses 4 cities from several US states, providing a plethora of different driving scenarios in a range of operating domains.
4. **Complexity:** The labelling provided is highly comprehensive - actors are labelled at great distances from the ego vehicle, with many active participants in each scene. Several complex scenes contain the presence of emergency vehicles (11 times more than the ROAD), six weather conditions (two times of ROAD), many lanes, busy roads, pedestrians and so on. Thus, ROAD-Waymo provides a considerably more challenging perception testbed than any other dataset of this kind.
5. **Verified Annotations:** Importantly, ROAD-Waymo is the first AV dataset guaranteed to be compliant with a set of commonsense constraints. Each annotation was automatically verified to be compliant with 251 domain-dependent logical requirements elicited for this task.
6. **ROAD++ domain adaptation framework:** The new ROAD-Waymo dataset is fully compatible with the original ROAD data. Together, they form the basis for a benchmarking framework for domain adaptation in autonomous driving (between two countries UK and the US and their 5 different cities), termed *ROAD++*.

**Tasks and Baselines:** Experiments were conducted to provide a benchmark for the following perception tasks:

1. Object/Agent, Action, and Event detection tasks using various types of models.
2. Cross-country (datasets) and cross-city real-to-real unsupervised domain adaptation for same tasks.
3. Neuro-symbolic prediction enhancement (*i.e.* the use of domain knowledge to guide the training of the neural models to ensure compliance with commonsense rules).

## 2 Related Work

**Autonomous Driving Datasets.** Autonomous vehicle perception has recently made significant progress, thanks to modern benchmarks that offer more diverse

environments and agent categories. For instance, previous datasets like NGSIM-180 [8] and highD [37] captured cars on highways using drones and surveillance cameras, while PIE [50] and JAAD [36] focused solely on pedestrian annotations using a single ego-vehicle camera. KITTI [20] was among the first to provide multimodal inputs, including camera frames and LiDAR point clouds, and annotations for both cars and pedestrians. Further down the line, Lyft [26], Waymo [13], nuScenes [4], Argoverse [65], Argoverse 2 [66], and Zenseact [1] provide large-scale, comprehensive annotation, HD-maps, odometer information and additional labels for other agents and environmental factors like weather and lighting conditions. A more recent dataset Rank2Tell [53] is designed for tasks involving both ranking the importance of various elements in a driving scenario and explaining those rankings.

However, these datasets focus on object detection, semantic segmentation or multi-object tracking tasks, lacking labels for high-level action understanding. Thus, there is no real competitor to our ROAD framework. A comprehensive comparison between the state-of-the-art datasets is shown in Table 1, with ROAD-Waymo and ROAD++ added for comparison.

**Table 1:** Features of the state-of-the-art autonomous vehicle datasets. "Man." means Manual and "Sem" means Semi. Hyphens “-” indicate that information is not available.

Dataset	KITTI	PIE	Lyft	nuScenes	Waymo-OM	LOKI	ROAD	Argoverse 2	Zenseact	Rank2Tell	ROAD-Waymo	ROAD++
Year of Release	2012	2019	2019	2019	2021	2021	2021	2023	2023	2024	2024	2024
# Classes	3	1	3	10	3	8	43	30	37	33	43	43
Night/Rain	X/X	X/X	✓/✓	✓/✓	✓/✓	✓/✓	✓/✓	X/X	X/✓	X/X	✓/✓	✓/✓
# Cities	1	1	1	2	6	-	3	6	14	1	3	4
Annotated Frames (k)	15	293	46	40	400	41	22	27k	100	23	198	320
Location Label	X	X	X	X	-	✓	✓	X	X	✓	✓	✓
Action Label	X	✓	X	✓	✓	✓	✓	X	X	X	✓	✓
Total Time (h)	1.5	6	1157	5.5	574	2.3	3	4.2	55.6	0.6	5.5	8.5
Download Size (Gb)	354	22	48	1400	-	4.2	16	58	-	-	18	34
Annotation	Man.	Auto	Man.	Auto	Man.	Man.	Auto	Man.	Man.	Man.	Sem.Auto	Sem.Auto

**Action and Event Detection Datasets** An action is a process - and, thus, temporal in nature. As such, datasets focusing on actions require detailed annotations in terms of both action labels and the localisation of the actions of interest as they evolve over time. Thus, the number of video datasets [23, 29, 59, 63] for action detection is much smaller than for other video tasks, e.g., action recognition [32]. AVA [23] is currently the largest action detection dataset, with 1.6M labels. Still, it suffers from a relative sparsity of the annotation, at one frame per second. MultiSport is a new multi-person dataset with spatiotemporally localised sports actions [40], featuring higher diversity, denser annotation and improved quality.

Most recently, [2] considered the detection of car-lane-change-events as a video action recognition problem. In the same vein, but for anomaly detection purposes, is the contribution of [64]. TITAN [46] provides annotations for pedestrians’ actions present in the road scene, but not for other road agents. PIE [50] also annotates 6 action classes for each road user for pedestrian behaviour anticipation. The annotation is focused on the pedestrian and the vehicles/traffic lights they interact with, and is thus quite sparse. All these datasets are promis-

ing and relevant: however, they are either sparsely annotated or limited in the number of labels and types (*e.g.* action or location) of labels, or both.

To the best of our knowledge, ROAD [57] is the only dataset in which the actions of all road users are densely annotated, including agent, action, and location labels.

**The ROAD Dataset.** The ROad event Awareness Dataset for Autonomous Driving (ROAD [57]) was originally designed to test event and action recognition and detection, being the first work to shift the focus from actions performed by human bodies to actions and events of agents. ROAD contains 22 8-minute long videos from the Oxford RobotCar Dataset [45] (OxRD), summing up to 122K frames. ROAD was introduced to provide event awareness capabilities, where each agent in the scene is annotated with road events for each bounding box, specifying the type of agent present in the bounding box, its action(s) and its location(s). The new annotations allowed for introducing new tasks such as spatiotemporal (i) agent detection, (ii) action detection, (iii) location detection, (iv) agent-action detection, (v) road event detection, and (vi) temporal segmentation of AV actions, all of which can be tested at frame and video levels. Moreover, these annotations can be leveraged for potential tasks, *e.g.* multi-object tracking, trajectory forecasting, action anticipation/prediction *etc.*

**Action Detection Methods.** Action detection encompasses two main classes of approaches. The first class [14, 15, 49, 62] involve using an auxiliary human detector to localise actors in keyframes, followed by action classification. These types of methods rely on models like Faster RCNN-R101-FPN [51] for human detection and RoIAlign [24, 33] for feature extraction. However, they may overlook contextual and interaction information outside the bounding box. The second class of approaches utilises end-to-end action detectors [6, 35, 60], which employ a single model to perform action detection. These methods simplify training by jointly training actor proposal networks and action classification networks. However, they also suffer from fixed RoI feature sampling. Recent advancements include one-stage action detectors such as MOC [41] and TubeR [71], which have their own limitations such as relying more on appearance features and neglecting multi-scale information.

Focusing on action detection in autonomous driving, [2, 34, 68] studied the trajectory and complex activities of cars in road scenarios. In [2] the focus was on detecting a specific action performed by a car - namely "lane change". To achieve this, models such as I3D, Spatiotemporal Multiplier ConvNet and Slowfast were trained to identify and classify the lane change action. [64] tackled anomaly detection for multiple actions in driving scenarios via a spatiotemporal graph auto-encoder, developed to learn normal driving behaviors using the trajectories of vehicles as input to the model. Inspired by end-to-end action detectors, in this study we also adopt 3D-RetinaNet [57] for road event detection.

**Unsupervised Domain Adaptation.** Unsupervised domain adaptation models are trained on a labelled source domain and adapted to an unlabelled target domain. There has been considerable progress towards bridging the domain gaps in major computer vision problems, including image classification [18, 44], seman-

tic segmentation [25, 27] and object detection [7, 39, 42]. Semantic and panoptic segmentation [54] are the most studied tasks for domain adaptation in autonomous driving setting [27]. Mostly, these problems are conducted in synthetic-to-real settings, where the source domain is synthetic (*e.g.* SYNTHIA [52]) but the target domain is real (*e.g.* [9]). However, few works consider real-to-real settings, and mostly in subdomain settings such as Day-to-Nighttime, Clear-to-Adverse-Weather [27, 28, 67],

Our proposed ROAD++ domain adaptation framework (making use of both ROAD and ROAD-Waymo) enables domain adaption and generalisation experiments between real datasets, considering both city and country locations. To the best of our knowledge, ROAD++ is the first real-to-real domain adaption benchmark for event awareness spanning two countries (UK *vs.* USA) and four different urban settings with drastically different road environments, *e.g.* left-hand *vs.* right-hand drive, narrow *vs.* wide roads *etc.*

### 3 ROAD-Waymo Dataset

ROAD-Waymo is a new, large-scale dataset providing a considerably more detailed, comprehensive and challenging playground for the development and test of advanced perception systems for autonomous vehicles. It has been designed to ensure compatibility with the existing ROAD (UK) dataset, and thus carries forward the same annotation strategy (Fig. 1) - this time applied to the popular Waymo dataset. It contains scenes from multiple US cities, with 8 times the number of annotated agent tubes when compared to ROAD. Importantly, for the first time a novel automated logical cross-checking process helps to ensure the integrity of the complex multi-label dataset.

**Table 2:** Comparison of ROAD (Oxford, UK) with the cities of ROAD-Waymo dataset.

Dataset Cities	ROAD Oxford, UK	ROAD-Waymo			
		Phoenix, USA	San Francisco, USA	Other	Total
Total duration (h)	3	2. (0.7x)	2.7 (0.9x)	0.7 (0.2x)	5.5 (1.8x)
Frames (K)	122	75 (0.6x)	98 (0.8x)	25 (0.20)	198 (1.6x)
Agent per Frame (Average)	5	16 (3.2x)	15 (3.0)	28 (5.6)	22 (4.4x)
Agent Tubes (K)	7	16 (2.3x)	5 (0.7x)	33 (4.7x)	54 (7.7x)
Agent Labels (K)	559	1,082 (1.9x)	2,723 (4.9x)	338 (0.6x)	4,143 (7.4x)
Action Labels (K)	641	1,146 (1.8x)	2,918 (4.5x)	361 (0.6x)	4,433 (6.9x)
Location Labels (K)	498	1,130 (2.3x)	2,804 (5.6x)	361 (0.7x)	4,296 (8.6x)
Event Labels (K)	548	880 (1.6x)	2,041 (3.7x)	269 (0.5x)	3,191 (5.8x)

#### 3.1 Style of annotation

Similarly to the ROAD dataset [57], three types of labels are used: *i)* *agents*, *e.g.*, cars, cyclists or pedestrians; *ii)* *actions*, *e.g.*, moving, turning or crossing;

and *iii) locations*, i.e., junction, incoming-lane or pavement. A complete list of all three types of labels is provided in the supplementary material. All of them are labelled from the ego vehicle (*i.e.* AV) point of view - as captured from the (front) camera installed upon the vehicle. In ROAD-Waymo we provide annotation for 12 agent classes, 30 action classes and 16 location classes. Different combinations of classes from these three label types yield a considerable number of *road events*. For instance, the road event “*Car is Moving in Vehicle lane*”, is composed of a triplet containing an agent (Car) performing an action (Moving) in a location (Vehicle-lane). A single agent may perform multiple actions, *e.g.* “*a car may be indicating left while turning left*” and be associated with multiple locations.

### 3.2 Annotation process

**Tracks and Boxes:** In ROAD-Waymo, all agents inherit bounding box and track annotation from the Waymo-Open dataset [61]. As bounding box and track annotation were not originally provided by Waymo for traffic lights, however, we added them using a YOLOv6 detector [38] for initialisation, to later manually filter or adjust the annotation.

**Labelling** was performed manually for all types of labels. Annotators labelled the agent type once per track, then propagated the labels in time for the entire track. Action and location labels were annotated at the start of the track, while class labels were added to or removed from frames whenever meaningful variations occurred.

**Annotation Verification.** Inspired by the core principles of software engineering, before starting with the annotation process we elicited a set of contextual “commonsense” requirements written in propositional logic and expressing facts that are always true in practice, such as “a traffic light cannot be red and green at the same time” or “an agent cannot move away and towards the vehicle at the same time”.<sup>9</sup> This allowed us to automatically check if *all* annotations were compliant with the requirements using a SAT solver<sup>10</sup>. All found violations were reported, and passed back to the annotators for further revision. This process was repeated (four times) until no more violations were found. Thanks to our SAT solver approach we were able to highlight and rectify 6,276 tubes annotations. See supplementary material for the list of different requirements and a visualisation of the annotation pipeline. ROAD-Waymo is the first dataset whose annotations are guaranteed to be compliant with a set of requirements, and it thus shares the same spirit of MLOps works such as [19, 21, 48], which advocate for a more structured approach to machine learning model development.

### 3.3 Statistics

ROAD-Waymo is considerably larger than the existing ROAD dataset (Table 2). It encompasses a greater number of agents, actions, and locations, with tubes

<sup>9</sup> To elicit the requirements, we adapted the propositional logic requirements from ROAD-R [22], resulting in a set of 251 requirements.

<sup>10</sup> We used the MINISAT solver. Link: <http://minisat.se>.

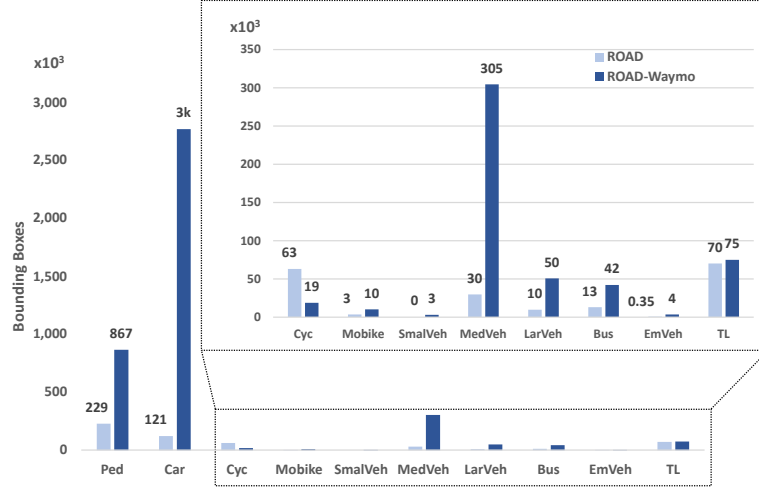
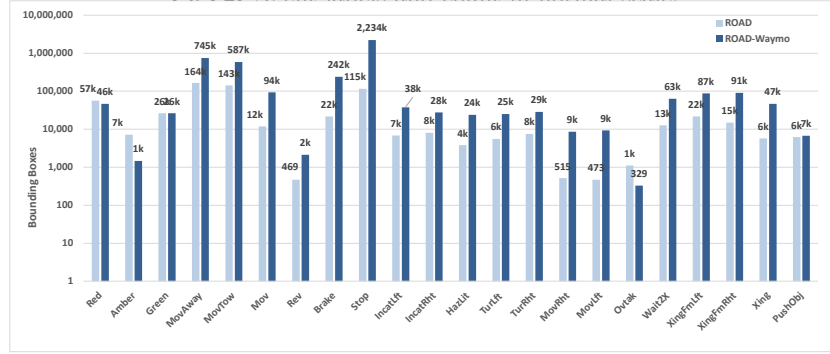
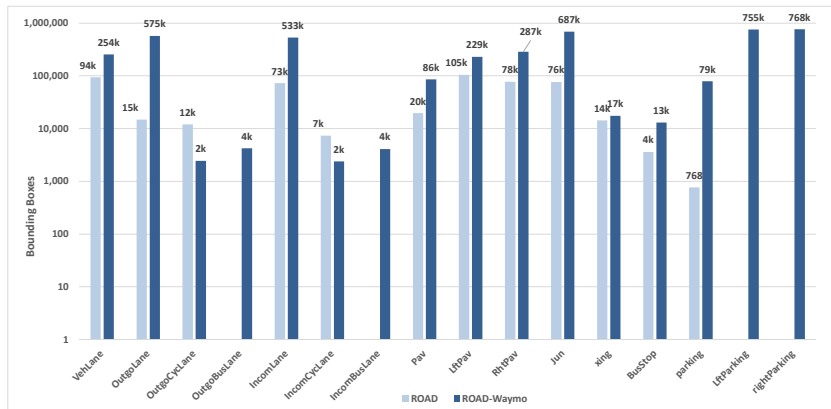


Fig. 2: Agent labels and count in normal scale

Fig. 3: Action labels and count in **logarithmic scale**. The full description of each abbreviation is provided in **Sup. Mat.**

and annotations averaging eight times the number. ROAD-Waymo exhibits a broader scope, encompassing four distinct (US) cities across six different weather conditions, while ROAD is confined to a single (UK) city, with half the range of weather conditions. As a general theme, ROAD-Waymo has many more vehicles (*e.g.* a stunning 30 times more cars, see Fig. 2) but fewer cyclists - just one example of a challenge encountered when shifting domain to another country. *Small-vehicle* and *Emergency-vehicle* had no instances at all in ROAD, while ROAD-Waymo contains more than 3K such instances. The presence of emergency situations is arguably extremely important to test the adaptation ability and safety of autonomous vehicles. Similar increments can be observed for other vehicle categories. Detailed visual comparisons between ROAD and ROAD-Waymo in terms of the number of Agents, Actions, and locations are shown in Figures 2, 3 and 4, respectively. Note that Figures 3 and 4 illustrate the comparison in logarithmic scale.





**Fig. 4:** Location labels and count in **logarithmic scale**. The full description of each abbreviation is provided in **Sup. Mat.**

## 4 Baselines

**3D-RetinaNet** [57] is designed for event detection in autonomous driving. Built upon the popular RetinaNet architecture (originally for object detection in 2D images), it leverages both spatial and temporal information to process video sequences - enabling detection and classification of actions. To process the input sequence of frames, it utilises a variety of 3D backbones (including Inflated 3D (I3D) [5] and SlowFast [16]) to capture hierarchical and multi-scale representations, which are used within two modules to capture and predict motion and temporal dynamics. Here, we update the 3D-RetinaNet to be trained on ROAD-Waymo and/or combined (ROAD + ROAD-Waymo) datasets.

**YOLOv8** [30] represents a highly advanced and top-of-the-line model that takes the accomplishments of previous YOLO iterations to new heights. It incorporates novel elements and enhancements that significantly enhance performance and adaptability, with its focus on speed, precision, and user-friendliness. Here, we train the YOLOv8 model for object (road agent) detection tasks.

**Domain Adaptation Baseline.** Reverse Gradient (RevGrad) [17] is a popular baseline approach to domain adaptation. This works by minimising the discrepancy between the source and target domains, by iteratively updating the model parameters such that the gradient of the adaptation loss with respect to the feature extractor is reversed during backpropagation - effectively aligning the feature distributions of the two domains. This encourages the model to learn domain-invariant representations that can generalise to the target domain, while retaining task-specific information from the source domain. In our tests, this model is trained on both domains UK ROAD and US ROAD-Waymo (source with labels, and target without labels), and then tested on the target domain (see Sec. 5.3).

**Neuro-Symbolic Baseline.** Commonsense, propositional logic requirements can be used for more than just checking annotation validity (as described above).

They also allow ROAD-Waymo to be utilised as a benchmark for neuro-symbolic models able to leverage the background knowledge expressed by these requirements to get better performance. To this end, we provide a neuro-symbolic baseline integrating the requirements in the loss, following a similar procedure as in ROAD-R [22]. This integration has been shown to improve the models’ performance in different works (*e.g.* [10–12]). The new loss measures the degree of constraint violation with respect to the neural predictions by mapping Boolean logic operators into differentiable algebraic operations, called t-norms [47]. Ultimately, this enhances neural network prediction by allowing the models access to background knowledge during training.

## 5 Experiments

### 5.1 Experimental Setup

**Tasks.** We follow the experimental setup of ROAD [57], and evaluate on ROAD-Waymo approaches over agent, action, location, duplex (joint label of agent+action) and event detection tasks, along with the temporal segmentation of the action performed by the AV itself. In addition, we introduce a set of experiments within the ROAD++ framework, where we study unsupervised domain adaption from one source dataset to a target dataset on the aforementioned tasks. In our tests, either ROAD or ROAD-Waymo play the role of the source dataset, with the other acting as target.

**Metrics.** Similarly to [57], in our experiments results are evaluated for both *frame-level* (bounding box) detection and *video-level* (tube) detection. As evaluation metrics we use frame mean Average Precision (f-mAP) and video mean Average Precision (video-mAP), respectively, commonly used in action detection [31, 55, 58]. The detection threshold for Intersection over Union (IoU) is set to 0.5 for f-mAP, indicating a 50% overlap between predicted and actual bounding boxes. To compute the video-mAP, instead, the results are evaluated on two IoU thresholds, namely, 0.2 (20% overlap) and 0.5 (50% overlap) as detecting tubes is more challenging than detecting single bounding boxes.

**Table 3:** ROAD-Waymo Frame-level results (f-mAP %) Val/Test.

Model	Agents	Actions	Locations	Duplexes	Events
I3D-08	15.7/16.7	12.3/13.9	<b>12.4/13.2</b>	10.5/10.1	6.2/5.3
I3D-32	15.4/15.2	12.2/13.0	12.3/12.8	10.4/9.4	6.3/5.6
SlowFast-08	16.1/15.3	<b>13.0/14.0</b>	11.9/12.4	<b>10.7/10.2</b>	4.7/5.7
SlowFast-32	16.0/15.0	<b>13.0/13.8</b>	11.9/12.2	<b>10.7/10.2</b>	<b>6.8/5.8</b>
YOLOv8	<b>38.1/31.6</b>	-/-	-/-	-/-	-/-

**Model training.** We train 3D-RetinaNet [57] with I3D [5] and SlowFast [16]. To train these models, we fix the input sequence to  $T = 8$  frames with an image size of  $600 \times 840$ . The backbone networks are initialised using weights from

Kinetics [32] pretraining. We employ an SGD optimizer with a step-learning rate, initially set to  $0.01 \times \text{number of GPUs}$  to then decrease by a factor of 10 after 18 and 25 epochs, totalling 30 epochs overall.

**Testing.** Although we train for 8 frame sequences, we can test the same network for longer input sequences as well. In our experiments we found that testing with 32 frames as input yielded slightly better results.

## 5.2 ROAD-Waymo Results

**Frame-Level Results.** Table 3 presents the frame-level results for all five tasks using f-mAP with an IoU threshold of 0.5. Results are reported for both validation and test sets separated by a forward slash (/). Rows in the Table represent combinations of feature extraction backbones (I3D and SlowFast) for the 3D-RetinaNet baseline. SlowFast with a test sequence length of 8 achieves the best performance for actions and duplex while, for events, SlowFast-32 reports the best performance.

We also report the performance of state-of-the-art YOLOv8 [30] for agent (object) detection, which indeed achieves the best performance for the task. The YOLOv8 model is trained and tested on a single frame rather than sequences, which is the main reason why we trialled it for agents only. Its remarkable performance is likely due to its use of several expedients such as: multi-scale training; mosaic data augmentation *etc.*

**Table 4:** ROAD-Waymo Video-level results (v-mAP %) Val/Test.

Model	Agents	Actions	Locations	Duplexes	Events
I3D-08	4.8/5.2	4.5/ <b>4.6</b>	4.2/6.1	6.2/5.7	4.2/ <b>4.3</b>
I3D-32	5.5/4.6	<b>4.6</b> /4.3	<b>4.4</b> / <b>6.2</b>	<b>6.2</b> /5.9	<b>4.7</b> /4.2
SlowFast-08	<b>6.5</b> / <b>5.5</b>	4.2/ <b>4.6</b>	4.2/5.4	5.9/ <b>6.3</b>	<b>4.7</b> / 4.1
SlowFast-32	6.4/5.1	4.1/4.4	4.3/4.7	5.5/6.1	4.3/4.0

**Video-Level Results.** Table 4 presents video-level results in terms of video-mAP. Results are reported for both 3D-RetinaNet backbones (I3D and SlowFast) and sequence lengths values (8 and 32 frames). Video-mAP is reported for IoU thresholds  $\delta$  of 0.2. SlowFast-08 reports the best performance for agents, actions, and duplex, while for locations and events I3D-32 and I3D-08 top the charts.

**Results of AV-Action Segmentation.** In addition to frame and tube detection, we also analyse the use of 3D-RetinaNet to temporally segment AV-action classes (Table 5). Results are reported for I3D and SlowFast backbones over both validation (Val) and test sets. The number of instances for each category is also provided - highlighting the complexity and challenge of recognising these categories in long-tail problems. The performance for the “AV-move” and “AV-stop” classes is high, likely because these two classes are predominantly represented in the dataset. The performance for the “turning” classes is reasonable, but the outcomes for the bottom two classes are notably poor. We can see that

**Table 5:** Temporal AV-action detection results

No instances		Frame-mAP@0.5 (%)	
Model		I3D	SlowFast
Eval subset	train / val / test	val / test	val / test
Move	88k / 29k / 30k	98.10 / 98.36	<b>98.11</b> / <b>98.46</b>
Stop	21k / 7.3k / 6.6k	94.78 / 95.89	<b>97.57</b> / <b>97.68</b>
Turn-right	1.8k / 0.8k / 1k	48.94 / 41.89	<b>59.30</b> / <b>48.40</b>
Turn-left	2.2k / 0.4k / 0.3k	31.98 / 47.24	<b>47.38</b> / <b>55.79</b>
Move-left	0.6k / 0.1k / 0.3k	<b>10.43</b> / <b>6.06</b>	6.74 / 4.86
Move-right	0.8k / 0.3k / 0.3k	3.65 / 14.58	<b>7.20</b> / <b>25.25</b>
Total/Mean	115k / 38k / 39k	47.99 / 50.67	<b>52.72</b> / <b>55.08</b>

SlowFast performs much better than I3D as it is more suited for classification problem.

### 5.3 ROAD++ framework (UK vs US Roads)

ROAD-Waymo has same annotation style as the original ROAD dataset, allowing us to study the problem of domain shift between UK and USA roads for AVs. We thus introduce a first-of-its-kind experimental setup for cross-dataset and cross-city real-to-real unsupervised domain adaptation, for the agent, action and event detection tasks.

**Cross dataset and cities evaluation.** We report a baseline for cross-dataset and cross-cities evaluation in Table 6, where I3D-based 3D-Retinanet is trained upon the train sets of ROAD, ROAD-Waymo, and ROAD++ (*i.e.* using together the training sets of both ROAD and ROAD-Waymo) separately. Then, each of the models is tested upon the test sets of all three mentioned datasets (where, again, the ROAD++ test set is the union of the test sets of the two datasets). Detailed f-mAP and v-mAP results are reported in Table 6. The IoU threshold was set to 0.5 for frame-mAP and to 0.2 for video-mAP. Three key findings arise from these results. Firstly, there is a significant reduction in the reported performance, exceeding a three-fold decrease, when training on ROAD and subsequently testing on ROAD-Waymo. Secondly, however, this does not hold when the reverse experiment is conducted. Lastly, it can be also observed the best results (as expected) are achieved when training on ROAD++ and testing it on individual test folds of ROAD and ROAD-Waymo.

**Unsupervised domain adaptation (UDA).** In adherence to the established practice in UDA, we conducted two more sets of experiments, in addition to the cross-dataset baseline described above and Table 6. The experiment was set up in the following manner: ROAD was chosen as source domain and ROAD-Waymo as target domain; evaluation was performed on target domain’s validation set. Whenever a model is trained on the source domain with labels it is referred to as “Lower bound”; when a model is trained on the target domain with labels it is referred to as “Upper bound”. UDA is the training setup

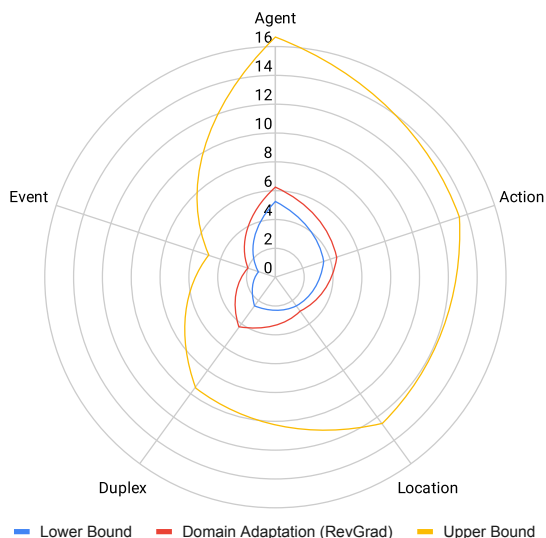


**Fig. 5:** Unsupervised domain adaptation results (frame-mAP % at IoU threshold of 0.5).

in which a model is trained on the source domain, with its labels, *and* on the target domain’s training set, but without labels.

Figure 5 illustrates how the results obtained using the Reverse Gradient (RevGrad) method (see Sec. 4) fall within the range delimited by the Lower and Upper bounds as defined above. The closeness of the baseline results to the Lower Bound indicates the potential of the ROAD++ family as a challenging real-world benchmark for developing and evaluating domain adaptation algorithms. Note that this is a real dataset-to-real dataset UDA setup, which makes it even more challenging than the more commonly considered synthetic-to-real setups in semantic segmentation [27].

#### 5.4 Neuro-symbolic Results

Finally, we experimented with two types of t-norms (Gödel and Łukasiewicz [47]) to compute to what extent the predictions satisfy the provided requirements, similarly to ROAD-R [22]. As our requirements have been written specifically for the agents, actions and locations detection, we eliminated the duplex and triplet detection tasks (originally considered in ROAD) from this set of experiments. The highest gains achieved with our method are reported for the location detection task when using the Gödel t-norm, as shown in Table 7, for the I3D model. Similar gains can be observed for SlowFast models, and can be consulted in supplementary material. Whilst a modest improvement, this comes at no additional cost in terms of labelling or data acquisition, provided that the annotations have been logically cross-checked.

**Table 6:** 3D-RetinaNet performance in cross-cities and countries (datasets) training and testing. Best results for each label type are in bold.

		Frame-mAP (%) @ IoU 0.5 / Video-mAP (%) @ IoU 0.2						
Train \ Test		Oxford	Phoenix	San Francisco	Other	ROAD-Waymo	ROAD++ (UK & US)	
ROAD (Oxford)	Agent	24.12 / 12.92	1.37 / 3.41	4.99 / 4.25	0.43 / 3.46	5.25 / 2.86	14.68 / 7.88	
	Action	<b>15.92</b> / 6.96	1.08 / 1.68	3.56 / 2.69	0.27 / 3.83	3.5 / 1.84	8.62 / 4.4	
	Location	<b>10.51</b> / 4.53	1.01 / 2.02	1.52 / 1.76	0.17 / 1.22	2.47 / 2.25	5.17 / 3.39	
Phoenix	Agent	6.18 / 6.30	4.09 / 2.79	5.75 / 3.08	0.93 / 4.65	10.64 / 2.97	8.41 / 4.63	
	Action	1.64 / 1.43	3.96 / <b>3.97</b>	4.39 / 2.46	0.97 / 5.54	9.19 / 2.98	5.41 / 2.20	
	Location	1.55 / 1.62	3.39 / 3.74	4.10 / 3.21	0.66 / 4.03	7.73 / 3.36	4.64 / 2.49	
San Francisco	Agent	10.94 / 7.73	3.09 / 2.14	10.35 / 5.19	1.14 / 5.54	14.42 / 3.96	12.68 / 5.84	
	Action	5.72 / 1.99	2.83 / 2.97	7.80 / 3.60	1.21 / 5.89	11.71 / 3.33	8.71 / 2.66	
	Location	3.99 / 2.36	2.63 / 4.06	7.92 / 4.82	0.78 / 5.08	11.03 / 4.23	7.51 / 3.29	
Other	Agent	6.36 / 5.46	2.06 / 1.39	4.27 / 2.70	0.71 / 2.99	6.82 / 2.07	6.59 / 3.76	
	Action	1.55 / 0.92	1.48 / 2.24	2.69 / 2.49	0.62 / 3.76	4.63 / 2.18	3.09 / 1.55	
	Location	2.55 / 1.39	1.89 / 2.74	3.63 / 3.25	0.52 / 4.08	5.82 / 2.89	4.18 / 2.14	
ROAD-Waymo	Agent	11.76 / 7.13	4.43 / 3.17	9.18 / 4.42	1.21 / 6.17	15.42 / 5.19	13.58 / 6.16	
	Action	3.94 / 1.95	4.18 / 3.96	7.38 / 3.80	1.18 / 6.26	13.0 / <b>4.58</b>	8.47 / 3.26	
	Location	3.98 / 2.40	3.92 / 7.09	7.42 / 4.40	0.94 / 4.31	<b>12.9</b> / <b>6.07</b>	8.44 / 4.23	
ROAD++ (UK & US)	Agent	<b>26.00</b> / <b>18.34</b>	<b>4.65</b> / <b>4.34</b>	<b>11.10</b> / <b>6.18</b>	<b>1.23</b> / <b>8.09</b>	<b>16.62</b> / <b>5.71</b>	<b>21.31</b> / <b>12.02</b>	
	Action	15.82 / <b>7.57</b>	<b>4.55</b> / 3.83	<b>8.88</b> / <b>4.23</b>	<b>1.26</b> / <b>7.25</b>	<b>13.39</b> / 4.32	<b>14.6</b> / <b>5.94</b>	
	Location	8.90 / <b>6.07</b>	4.28 / <b>7.74</b>	<b>8.93</b> / <b>5.23</b>	<b>0.96</b> / <b>5.95</b>	12.57 / 4.22	<b>10.73</b> / <b>5.14</b>	

**Table 7:** Baseline *vs.* t-norm-based loss models, using I3D. Frame-level (mAP %) are calculated on ROAD-Waymo val/test sets.

Model	Agents	Actions	Locations
I3D	19.05 / 19.61	14.80 / 16.00	15.31 / 15.72
+ Gödel	<b>19.70</b> / <b>19.96</b>	<b>15.59</b> / 15.66	<b>16.03</b> / <b>16.89</b>
+ Łukasiewicz	18.07 / 19.89	15.13 / <b>16.13</b>	15.37 / 15.84

Our method provides an essentially free performance enhancement and opens up further research directions for using domain knowledge during training in complex perception tasks and real-world scenarios.

## 6 Conclusions

The ROAD-Waymo dataset presented in this paper has been designed to enable the development of autonomous vehicle perception systems capable of advancing beyond object detection, and explore the ability to truly *understand* what is happening around the vehicle. ROAD-Waymo is a large-scale dataset for activity and event detection and prediction - encompassing approximately 200k comprehensively labelled driving scenarios, spanning 4 different US cities, in 6 different (labelled) weather conditions. The integrity of the dataset has been confirmed and enhanced using a novel context-aware automated validation approach, allowing the identification and correction of thousands of potential human labelling errors. This opens the door to tackling challenging perception problems including “present time” tasks such as event, agent and action detection, as well as “future time” prediction tasks such as action anticipation, trajectory prediction and so on. Detailed baselines have been provided for the first set of tasks.

As the (US) ROAD-Waymo is fully compatible with the original (UK) ROAD dataset, pairing the two datasets together forms the basis for a new ROAD++ family of datasets usable for the development and real-world testing of domain adaptation techniques - for which a baseline is also provided. Finally, as the



dataset comes with commonsense logical requirements, it can be used to develop and test neuro-symbolic methods for enhancing the neural networks’ predictions. A baseline is also provided for this purpose.

ROAD-Waymo has been shown to present a significant challenge compared to existing datasets for this purpose, highlighting the scale of the work on AV perception still required to enable safe real-world driving. The ROAD++ family of datasets and challenges provides the perfect playground to enable the wider community to develop and push the boundaries of new approaches and methods for action and event detection in autonomous driving, and domain adaptation between countries.

**Future work.** The dataset in its present form comes with data streams in other modalities (*e.g.* LIDAR and GPS attached to each video), providing the potential for future expansion of the labelling into true multi-modal labels. Another intriguing possibility is to project the road event annotation into the 3D space in the form of 3D detections, where LIDAR and camera calibration is available. In terms of results, the performance of the baselines provided is low for long-tail classes. We only used focal-loss [43] to handle this problem without any explicit class balancing efforts, so more work needs to be done there.

## Acknowledgements

This project has received funding from the European Union’s Horizon 2020 research and innovation programme, under grant agreement No. 964505 (E-pi). The project has also received funding from the Leverhulme Trust, Research Project Grant RPG-2019-243.

## References

1. Alibeigi, M., Ljungbergh, W., Tonderski, A., Hess, G., Lilja, A., Lindström, C., Motorniuk, D., Fu, J., Widahl, J., Petersson, C.: Zenseact open dataset: A large-scale and diverse multimodal dataset for autonomous driving. In: Proceedings of the IEEE/CVF International Conference on Computer Vision (ICCV). pp. 20178–20188 (October 2023) [4](#)
2. Biparva, M., Fernández-Llorca, D., Gonzalo, R.I., Tsotsos, J.K.: Video action recognition for lane-change classification and prediction of surrounding vehicles. *IEEE Transactions on Intelligent Vehicles* **7**(3), 569–578 (2022). <https://doi.org/10.1109/TIV.2022.3164507> [4](#), [5](#)
3. Caesar, H., Bankiti, V., Lang, A.H., Vora, S., Liong, V.E., Xu, Q., Krishnan, A., Pan, Y., Baldan, G., Beijbom, O.: nuscenes: A multimodal dataset for autonomous driving. arXiv preprint arXiv:1903.11027 (2019) [23](#)
4. Caesar, H., Bankiti, V., Lang, A.H., Vora, S., Liong, V.E., Xu, Q., Krishnan, A., Pan, Y., Baldan, G., Beijbom, O.: nuscenes: A multimodal dataset for autonomous driving. In: Proceedings of the IEEE/CVF conference on computer vision and pattern recognition. pp. 11621–11631 (2020) [4](#)
5. Carreira, J., Zisserman, A.: Quo vadis, action recognition? a new model and the kinetics dataset. In: proceedings of the IEEE Conference on Computer Vision and Pattern Recognition. pp. 6299–6308 (2017) [9](#), [10](#)

6. Chen, S., Sun, P., Xie, E., Ge, C., Wu, J., Ma, L., Shen, J., Luo, P.: Watch only once: An end-to-end video action detection framework. In: Proceedings of the IEEE/CVF International Conference on Computer Vision. pp. 8178–8187 (2021) [5](#)
7. Chen, Y., Wang, H., Li, W., Sakaridis, C., Dai, D., Van Gool, L.: Scale-aware domain adaptive faster r-cnn. *International Journal of Computer Vision* **129**(7), 2223–2243 (2021) [6](#)
8. Coifman, B., Li, L.: A critical evaluation of the next generation simulation (ngsim) vehicle trajectory dataset. *Transportation Research Part B: Methodological* **105**, 362–377 (2017). <https://doi.org/https://doi.org/10.1016/j.trb.2017.09.018>, <https://www.sciencedirect.com/science/article/pii/S0191261517300838> [4](#)
9. Cordts, M., Omran, M., Ramos, S., Rehfeld, T., Enzweiler, M., Benenson, R., Franke, U., Roth, S., Schiele, B.: The cityscapes dataset for semantic urban scene understanding. In: Proceedings of the IEEE conference on computer vision and pattern recognition. pp. 3213–3223 (2016) [1](#), [6](#)
10. Diligenti, M., Gori, M., Sacca, C.: Semantic-based regularization for learning and inference. *Art. Intell.* **244** (2017) [10](#)
11. Diligenti, M., Roychowdhury, S., Gori, M.: Integrating prior knowledge into deep learning. In: Proc. of ICMLA (2017) [10](#)
12. Donadello, I., Serafini, L., d’Avila Garcez, A.: Logic tensor networks for semantic image interpretation. In: Proc. of IJCAI (2017) [10](#)
13. Ettinger, S., Cheng, S., Caine, B., Liu, C., Zhao, H., Pradhan, S., Chai, Y., Sapp, B., Qi, C.R., Zhou, Y., et al.: Large scale interactive motion forecasting for autonomous driving: The waymo open motion dataset. In: Proceedings of the IEEE/CVF International Conference on Computer Vision. pp. 9710–9719 (2021) [4](#)
14. Fan, H., Xiong, B., Mangalam, K., Li, Y., Yan, Z., Malik, J., Feichtenhofer, C.: Multiscale vision transformers. In: Proceedings of the IEEE/CVF International Conference on Computer Vision. pp. 6824–6835 (2021) [5](#)
15. Faure, G.J., Chen, M.H., Lai, S.H.: Holistic interaction transformer network for action detection. In: Proceedings of the IEEE/CVF Winter Conference on Applications of Computer Vision. pp. 3340–3350 (2023) [5](#)
16. Feichtenhofer, C., Fan, H., Malik, J., He, K.: Slowfast networks for video recognition. In: Proceedings of the IEEE international conference on computer vision. pp. 6202–6211 (2019) [9](#), [10](#)
17. Ganin, Y., Lempitsky, V.: Unsupervised domain adaptation by backpropagation. In: International conference on machine learning. pp. 1180–1189. PMLR (2015) [9](#)
18. Ganin, Y., Ustinova, E., Ajakan, H., Germain, P., Larochelle, H., Laviolette, F., Marchand, M., Lempitsky, V.: Domain-adversarial training of neural networks. *The journal of machine learning research* **17**(1), 2096–2030 (2016) [5](#)
19. Gebru, T., Morgenstern, J., Vecchione, B., Vaughan, J.W., Wallach, H.M., III, H.D., Crawford, K.: Datasheets for datasets. *CoRR* **abs/1803.09010** (2018), <http://arxiv.org/abs/1803.09010> [7](#)
20. Geiger, A., Lenz, P., Urtasun, R.: Are we ready for autonomous driving? the kitti vision benchmark suite. In: 2012 IEEE Conference on Computer Vision and Pattern Recognition. pp. 3354–3361 (2012). <https://doi.org/10.1109/CVPR.2012.6248074> [1](#), [4](#)
21. Giunchiglia, E., Imrie, F., van der Schaar, M., Lukasiewicz, T.: Machine learning with requirements: a manifesto (2023) [7](#)

22. Giunchiglia, E., Stoian, M.C., Khan, S., Cuzzolin, F., Lukasiewicz, T.: ROAD-R: The autonomous driving dataset for learning with requirements. *Machine Learning Journal* (2023) [2](#), [7](#), [10](#), [13](#), [25](#)
23. Gu, C., Sun, C., Vijayanarasimhan, S., Pantofaru, C., Ross, D.A., Toderici, G., Li, Y., Ricco, S., Sukthankar, R., Schmid, C., et al.: Ava: A video dataset of spatio-temporally localized atomic visual actions. *arXiv preprint arXiv:1705.08421* (2017) [4](#)
24. He, K., Gkioxari, G., Dollár, P., Girshick, R.: Mask r-cnn. In: *Proceedings of the IEEE international conference on computer vision*. pp. 2961–2969 (2017) [5](#)
25. Hoffman, J., Wang, D., Yu, F., Darrell, T.: Fcns in the wild: Pixel-level adversarial and constraint-based adaptation. *arXiv preprint arXiv:1612.02649* (2016) [6](#)
26. Houston, J., Zuidhof, G., Bergamini, L., Ye, Y., Chen, L., Jain, A., Omari, S., Iglovikov, V., Ondruska, P.: One thousand and one hours: Self-driving motion prediction dataset. *arXiv preprint arXiv:2006.14480* (2020) [4](#)
27. Hoyer, L., Dai, D., Van Gool, L.: Daformer: Improving network architectures and training strategies for domain-adaptive semantic segmentation. In: *Proceedings of the IEEE/CVF Conference on Computer Vision and Pattern Recognition*. pp. 9924–9935 (2022) [6](#), [13](#)
28. Hoyer, L., Dai, D., Van Gool, L.: Domain adaptive and generalizable network architectures and training strategies for semantic image segmentation. *arXiv preprint arXiv:2304.13615* (2023) [6](#)
29. Jhuang, H., Gall, J., Zuffi, S., Schmid, C., Black, M.J.: Towards understanding action recognition. In: *Proceedings of the IEEE International Conference on Computer Vision (ICCV)*. pp. 3192–3199 (2013) [4](#)
30. Jocher, G., Chaurasia, A., Qiu, J.: YOLO by Ultralytics (Jan 2023), <https://github.com/ultralytics/ultralytics> [9](#), [11](#)
31. Kalogeiton, V., Weinzaepfel, P., Ferrari, V., Schmid, C.: Action tubelet detector for spatio-temporal action localization. In: *ICCV* (2017) [10](#)
32. Kay, W., Carreira, J., Simonyan, K., Zhang, B., Hillier, C., Vijayanarasimhan, S., Viola, F., Green, T., Back, T., Natsev, P., others et al.: The kinetics human action video dataset. *arXiv preprint arXiv:1705.06950* (2017) [4](#), [11](#)
33. Khan, S., Cuzzolin, F.: Spatiotemporal deformable scene graphs for complex activity detection. *arXiv preprint arXiv:2104.08194* (2021) [5](#)
34. Khan, S., Teeti, I., Bradley, A., Elhoseiny, M., Cuzzolin, F.: A hybrid graph network for complex activity detection in video. In: *Proceedings of the IEEE/CVF Winter Conference on Applications of Computer Vision*. pp. 6762–6772 (2024) [5](#)
35. Köpüklü, O., Wei, X., Rigoll, G.: You only watch once: A unified cnn architecture for real-time spatiotemporal action localization. *arXiv preprint arXiv:1911.06644* (2019) [5](#)
36. Kotseruba, I., Rasouli, A., Tsotsos, J.K.: Joint attention in autonomous driving (jaad). *arXiv preprint arXiv:1609.04741* (2016) [4](#)
37. Krajewski, R., Bock, J., Kloeker, L., Eckstein, L.: The highd dataset: A drone dataset of naturalistic vehicle trajectories on german highways for validation of highly automated driving systems. In: *21st International Conference on Intelligent Transportation Systems (ITSC)*. pp. 2118–2125 (2018). <https://doi.org/10.1109/ITSC.2018.8569552> [4](#)
38. Li, C., Li, L., Jiang, H., Weng, K., Geng, Y., Li, L., Ke, Z., Li, Q., Cheng, M., Nie, W., et al.: Yolov6: A single-stage object detection framework for industrial applications. *arXiv preprint arXiv:2209.02976* (2022) [7](#)

39. Li, W., Liu, X., Yuan, Y.: Sigma: Semantic-complete graph matching for domain adaptive object detection. In: Proceedings of the IEEE/CVF Conference on Computer Vision and Pattern Recognition. pp. 5291–5300 (2022) [6](#)
40. Li, Y., Chen, L., He, R., Wang, Z., Wu, G., Wang, L.: Multisports: A multi-person video dataset of spatio-temporally localized sports actions. In: Proceedings of the IEEE/CVF International Conference on Computer Vision. pp. 13536–13545 (2021) [4](#)
41. Li, Y., Wang, Z., Wang, L., Wu, G.: Actions as moving points. arXiv preprint arXiv:2001.04608 (2020) [5](#)
42. Li, Y.J., Dai, X., Ma, C.Y., Liu, Y.C., Chen, K., Wu, B., He, Z., Kitani, K., Vajda, P.: Cross-domain adaptive teacher for object detection. In: Proceedings of the IEEE/CVF Conference on Computer Vision and Pattern Recognition. pp. 7581–7590 (2022) [6](#)
43. Lin, T.Y., Goyal, P., Girshick, R., He, K., Dollár, P.: Focal loss for dense object detection. In: Proceedings of the IEEE international conference on computer vision. pp. 2980–2988 (2017) [15](#)
44. Long, M., Cao, Z., Wang, J., Jordan, M.I.: Conditional adversarial domain adaptation. *Advances in neural information processing systems* **31** (2018) [5](#)
45. Maddern, W., Pascoe, G., Linegar, C., Newman, P.: 1 Year, 1000km: The Oxford RobotCar Dataset. *The International Journal of Robotics Research (IJRR)* **36**(1), 3–15 (2017). <https://doi.org/10.1177/0278364916679498>, <http://dx.doi.org/10.1177/0278364916679498> [1](#), [5](#)
46. Malla, S., Dariush, B., Choi, C.: Titan: Future forecast using action priors. In: Proceedings of the IEEE/CVF Conference on Computer Vision and Pattern Recognition. pp. 11186–11196 (2020) [4](#)
47. Metcalfe, G.: Fundamentals of fuzzy logics. <https://www.logic.at/tbilisi05/Metcalfe-notes.pdf> (2005) [10](#), [13](#), [25](#)
48. Mitchell, M., Wu, S., Zaldivar, A., Barnes, P., Vasserman, L., Hutchinson, B., Spitzer, E., Raji, I.D., Gebru, T.: Model cards for model reporting. *CoRR abs/1810.03993* (2018), <http://arxiv.org/abs/1810.03993> [7](#)
49. Pan, J., Chen, S., Shou, M.Z., Liu, Y., Shao, J., Li, H.: Actor-context-actor relation network for spatio-temporal action localization. In: Proceedings of the IEEE/CVF Conference on Computer Vision and Pattern Recognition. pp. 464–474 (2021) [5](#)
50. Rasouli, A., Kotseruba, I., Kunic, T., Tsotsos, J.: Pie: A large-scale dataset and models for pedestrian intention estimation and trajectory prediction. In: 2019 IEEE/CVF International Conference on Computer Vision (ICCV). pp. 6261–6270 (2019). <https://doi.org/10.1109/ICCV.2019.00636> [4](#)
51. Ren, S., He, K., Girshick, R., Sun, J.: Faster r-cnn: Towards real-time object detection with region proposal networks. *Advances in neural information processing systems* **28** (2015) [5](#)
52. Ros, G., Sellart, L., Materzynska, J., Vazquez, D., Lopez, A.M.: The synthia dataset: A large collection of synthetic images for semantic segmentation of urban scenes. In: Proceedings of the IEEE conference on computer vision and pattern recognition. pp. 3234–3243 (2016) [6](#)
53. Sachdeva, E., Agarwal, N., Chundi, S., Roelofs, S., Li, J., Kochenderfer, M., Choi, C., Dariush, B.: Rank2tell: A multimodal driving dataset for joint importance ranking and reasoning. In: Proceedings of the IEEE/CVF Winter Conference on Applications of Computer Vision. pp. 7513–7522 (2024) [4](#)
54. Saha, S., Hoyer, L., Obukhov, A., Dai, D., Van Gool, L.: Edaps: Enhanced domain-adaptive panoptic segmentation. arXiv preprint arXiv:2304.14291 (2023) [6](#)

55. Saha, S., Singh, G., Sapienza, M., Torr, P.H., Cuzzolin, F.: Deep learning for detecting multiple space-time action tubes in videos. arXiv preprint arXiv:1608.01529 (2016) [10](#)
56. Sakaridis, C., Dai, D., Van Gool, L.: Acdc: The adverse conditions dataset with correspondences for semantic driving scene understanding. In: Proceedings of the IEEE/CVF International Conference on Computer Vision. pp. 10765–10775 (2021) [1](#)
57. Singh, G., Akrigg, S., Di Maio, M., Fontana, V., Alitappeh, R.J., Saha, S., Jeddissaravi, K., Yousefi, F., Culley, J., Nicholson, T., et al.: Road: The road event awareness dataset for autonomous driving. IEEE Transactions on Pattern Analysis & Machine Intelligence (01), 1–1 (feb 5555). <https://doi.org/10.1109/TPAMI.2022.3150906> [1](#), [2](#), [5](#), [6](#), [9](#), [10](#), [20](#)
58. Singh, G., Saha, S., Sapienza, M., Torr, P., Cuzzolin, F.: Online real-time multiple spatiotemporal action localisation and prediction. In: Proceedings of the IEEE Conference on Computer Vision and Pattern Recognition. pp. 3637–3646 (2017) [10](#)
59. Soomro, K., Zamir, A.R., Shah, M.: Ucf101: A dataset of 101 human actions classes from videos in the wild (2012) [4](#)
60. Sun, C., Shrivastava, A., Vondrick, C., Murphy, K., Sukthankar, R., Schmid, C.: Actor-centric relation network. In: Proceedings of the European Conference on Computer Vision (ECCV). pp. 318–334 (2018) [5](#)
61. Sun, P., Kretschmar, H., Dotiwalla, X., Chouard, A., Patnaik, V., Tsui, P., Guo, J., Zhou, Y., Chai, Y., Caine, B., et al.: Scalability in perception for autonomous driving: Waymo open dataset. In: Proceedings of the IEEE/CVF conference on computer vision and pattern recognition. pp. 2446–2454 (2020) [2](#), [3](#), [7](#)
62. Tong, Z., Song, Y., Wang, J., Wang, L.: Videomae: Masked autoencoders are data-efficient learners for self-supervised video pre-training. arXiv preprint arXiv:2203.12602 (2022) [5](#)
63. Weinzaepfel, P., Martin, X., Schmid, C.: Human action localization with sparse spatial supervision. arXiv preprint arXiv:1605.05197 (2016) [4](#)
64. Wiederer, J., Bouazizi, A., Troina, M., Kressel, U., Belagiannis, V.: Anomaly detection in multi-agent trajectories for automated driving. In: Faust, A., Hsu, D., Neumann, G. (eds.) Proceedings of the 5th Conference on Robot Learning. Proceedings of Machine Learning Research, vol. 164, pp. 1223–1233. PMLR (08–11 Nov 2022) [4](#), [5](#)
65. Wilson, B., Qi, W., Agarwal, T., Lambert, J., Singh, J., Khandelwal, S., Pan, B., Kumar, R., Hartnett, A., Pontes, J.K., et al.: Argoverse 2: Next generation datasets for self-driving perception and forecasting. arXiv preprint arXiv:2301.00493 (2023) [1](#), [4](#)
66. Wilson, B., Qi, W., Agarwal, T., Lambert, J., Singh, J., Khandelwal, S., Pan, B., Kumar, R., Hartnett, A., Pontes, J.K., et al.: Argoverse 2: Next generation datasets for self-driving perception and forecasting. arXiv preprint arXiv:2301.00493 (2023) [4](#)
67. Wu, X., Wu, Z., Guo, H., Ju, L., Wang, S.: Dannet: A one-stage domain adaptation network for unsupervised nighttime semantic segmentation. In: Proceedings of the IEEE/CVF Conference on Computer Vision and Pattern Recognition. pp. 15769–15778 (2021) [6](#)
68. Yao, Y., Wang, X., Xu, M., Pu, Z., Wang, Y., Atkins, E., Crandall, D.: Dota: unsupervised detection of traffic anomaly in driving videos. IEEE transactions on pattern analysis and machine intelligence (2022) [5](#)

69. Yu, F., Chen, H., Wang, X., Xian, W., Chen, Y., Liu, F., Madhavan, V., Darrell, T.: Bdd100k: A diverse driving dataset for heterogeneous multitask learning. In: Proceedings of the IEEE/CVF conference on computer vision and pattern recognition. pp. 2636–2645 (2020) [1](#)
70. Yu, L., Qian, Y., Liu, W., Hauptmann, A.G.: Argus++: Robust real-time activity detection for unconstrained video streams with overlapping cube proposals. In: Proceedings of the IEEE/CVF Winter Conference on Applications of Computer Vision. pp. 112–121 (2022) [2](#)
71. Zhao, J., Zhang, Y., Li, X., Chen, H., Shuai, B., Xu, M., Liu, C., Kundu, K., Xiong, Y., Modolo, D., et al.: Tuber: Tubelet transformer for video action detection. In: Proceedings of the IEEE/CVF Conference on Computer Vision and Pattern Recognition. pp. 13598–13607 (2022) [5](#)

## Supplementary Materials

### 7 Additional Details

#### 7.1 Labels

In this section we include the list of labels that we used to annotate the bounding boxes. The list of labels can be found in Table 8. In the Table, we include in parenthesis the abbreviated name for each label (such abbreviation will be used in the remaining sections). The detailed description of each label can be found the supplementary materials of ROAD<sup>11</sup> [57].

<b>Agents:</b>	Pedestrian (Ped), Car (Car), Cyclist (Cyc), Motorbike (Mobike), Small Vehicle (SmalVeh) Medium vehicle (MedVeh), Large vehicle (LarVeh), Bus (Bus), Emergency vehicle (EmVeh), Traffic light (TL).
<b>Actions:</b>	Move away (MovAway), Move towards (MovTow), Move (Mov), Reverse (Rev) Brake (Brake), Stop (Stop), Indicating left (IncatLft), Indicating right (IncatRht), Hazards lights on (HazLit), Turn left (TurLft), Turn right (TurRht), Move right (MovRht), Move left (MovLft), Overtake (Ovtak), Wait to cross (Wait2X), Cross from left (XingFmLft), Cross from right, Crossing (XingFmRht), Crossing (Xing), Push object (PushObj), Red Traffic Light (Red), Amber Traffic Light (Amber), Green Traffic Light (Green).
<b>Locations:</b>	Autonomous vehicle lane (AV lane), Outgoing lane (OutgoLane), Outgoing cycle lane (OutgoCycLane), Outgoing bus lane (OutgoBusLane), Incoming lane (IncomLane), Incoming cycle lane (IncomCycLane), Incoming bus Lane (IncomBusLane), Pavement (Pav), Left pavement (LftPav), Right pavement (RhtPav), Junction (Jun), Crossing location (xing), Bus stop (BusStop), Parking (parking), Left parking (LftParking), Right parking (RhtParking).

**Table 8:** ROAD-Waymo list of labels and their abbreviation.

<sup>11</sup> <http://export.arxiv.org/pdf/2102.11585>



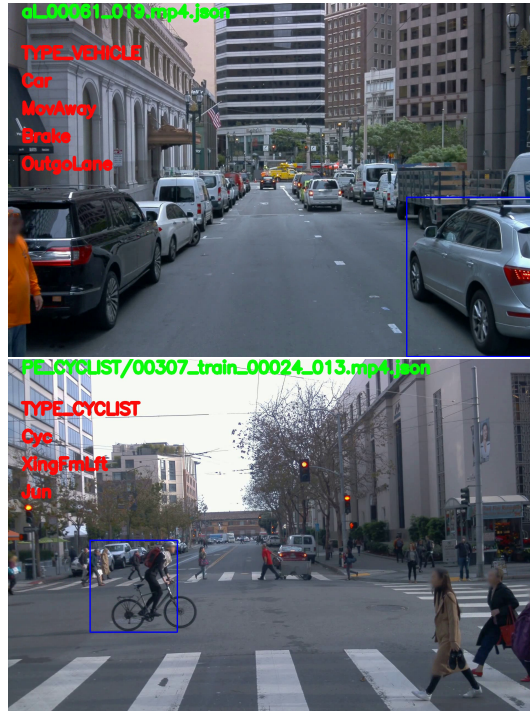


Fig. 6: An example of labels for a vehicle and cyclist.

## 7.2 Annotation examples

In Fig. 6, two different scenarios are shown. In the left panel a car is *moving away* from the AV in the *outgoing lane* while the *brake* light is on. In the right panel, a bicycle (or *cyclist*) is moving from left to right, we call it "*crossing from left to right*" in a *junction*. It should be noticed that, for simplification, we consider a single agent in each image.

## 7.3 Annotation check pipeline

As specified in the main body of the paper, we assisted the manual checking performed by the annotators by verifying whether the annotations satisfy a set of contextual ‘commonsense’ requirements. In order to elicit the requirements, we adapted the 243 propositional logic requirements present in ROAD-R to ROAD-Waymo by adding 55 novel requirements and removing 47 non-compatible ones. We obtained a total 251 requirements. In Table 9 we list the requirements we added to the ROAD-R set, while in Table 10 we list the removed ones. The requirements are written using the set-based notation used in ROAD-R, in which each set represents a disjunction over possibly negated atoms. Thus, for example, the requirement “{neg Car, neg SmalVeh}” can be expressed in propositional

logic as  $(\neg \text{Car} \vee \neg \text{SmallVeh})$  and states the fact that an agent cannot be a car and a small vehicle at the same time. The difference in the set of requirements are due to the fact that ROAD and ROAD-Waymo use two slightly different set of labels (e.g., SmalVeh is used in ROAD-Waymo but not in ROAD).

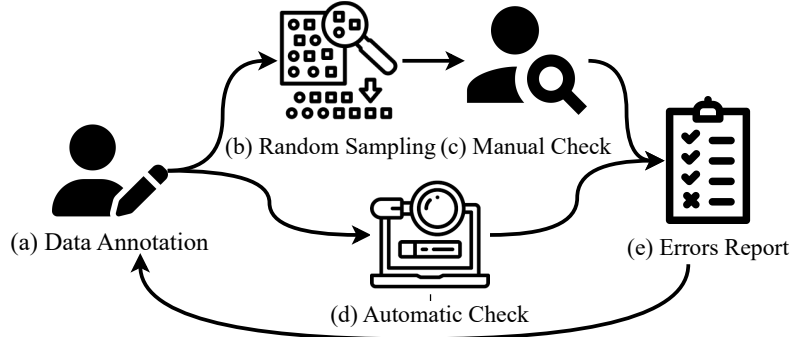


**Fig. 7:** Annotations check pipeline.

In Figure 7 we present our circular five-step ((a)-(e)) annotation checking pipeline, combining manual and automated checks to refine the labelling process. More precisely, (a) the annotators first label the videos, then (b) a subset of videos are randomly sampled to (c) be assessed by a member of our team. At the same time, (d) we automatically check if *all* annotations are compliant with the requirements using a SAT solver<sup>12</sup>. All the manually- and automatically-found violations are then (e) collected in a single report and passed to the annotators for further revision. We repeated this process four times (until no more violations were found) and ultimately found and corrected the annotations of a total of 6276 tubes with the help of the SAT solver.

#### 7.4 Multi-Modality Data

Our ROAD-Waymo is fully compatible and synchronised with the 3D-point cloud data provided in the official open Waymo dataset<sup>13</sup> (illustrated in Figure 8). However, it is important to note that in our ROAD-Waymo, our focus is solely on the bounding boxes of the frontal view for event detection, as we have annotated only the frontal view for this purpose.

<sup>12</sup> We used the MINISAT solver. Link: <http://minisat.se>.

<sup>13</sup> <https://waymo.com/open/data/perception/>

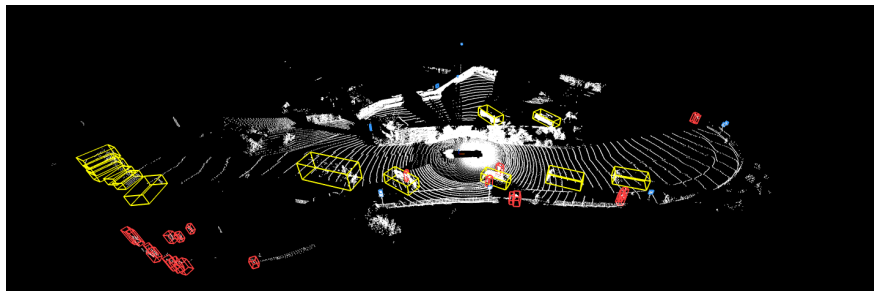


**Fig. 8:** Waymo open dataset 3D-point cloud visualisation.

## 8 Additional Results

### 8.1 Experimental Details

All the experiments are performed using a max of GPU servers including  $8 \times$  Nvidia-A30 with 24GB onboard memory (VRAM),  $8 \times$  Nvidia-RTX 6000 with 24GB VRAM, and  $3 \times$  Nvidia-A100 with 80GB VRAM. To ensure a fair comparison of the results, consistent hyperparameters, as specified in the main paper, were maintained across all the servers.

### 8.2 Inference on NuScenes

To demonstrate the effectiveness of our ROAD++ domain adaptation framework, we present inferences on another distinct autonomous driving dataset known as the NuScenes dataset<sup>14</sup> [3]. The results, illustrated in Figure 9, involve randomly selected frames at varying intervals for models trained on all three datasets (ROAD, ROAD-Waymo, and ROAD++). The outcomes reveal that the model trained on ROAD++ exhibits fewer misdetections and more accurate event detection labels compared to the other two datasets.

### 8.3 ROAD-Waymo Class-wise

In this section, we also present class-wise detection results of ROAD-Waymo for all label types. All the results are generated for the frame and video level results on the test set. Table 11 shows the detailed results for individual labels. For duplex labels, the class-wise and split-wise results can be found in Table 12, while Table 13 presents the corresponding outcomes for event labels.

### 8.4 Neuro-symbolic results for SlowFast

In order to test whether logical requirements capturing background knowledge can help the neural networks learn better during training, we incorporated the

<sup>14</sup> <https://www.nuscenes.org/>

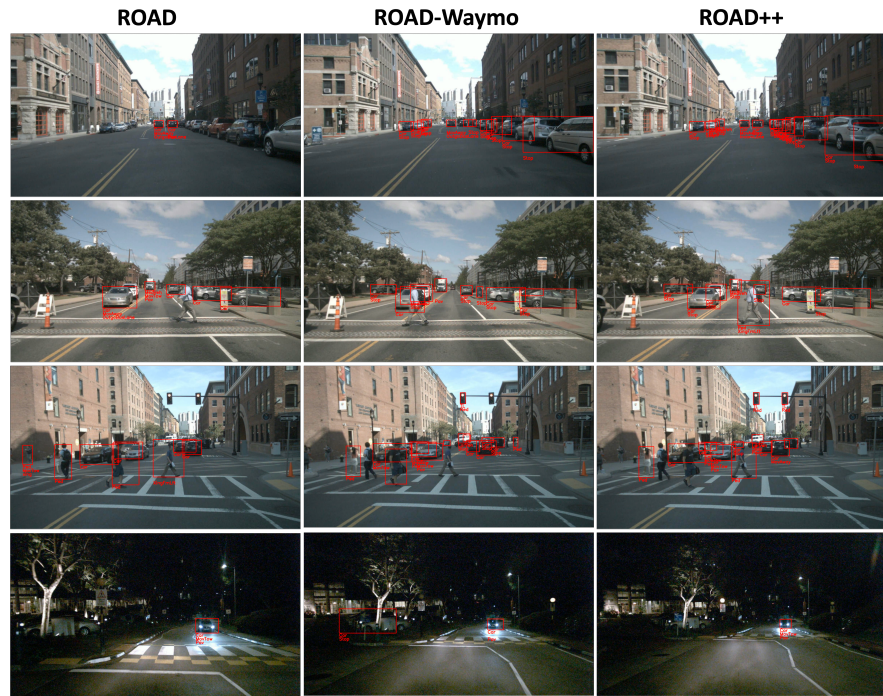


**Fig. 9:** Visualisation of inferences on the NuScenes dataset for models trained on ROAD, ROAD-Waymo, and ROAD++.

requirements into a new t-norm-based loss term of 3D-RetinatNet models using an I3D- and a SlowFast-based backbone. We experimented with two types of t-norms (Gödel and Łukasiewicz [47]) to compute to what extent the predictions satisfy the provided requirements, similarly to ROAD-R [22].

The results for SlowFast in Table 14 are consistent with our observations from the I3D case, presented in Table 6 from the paper, and show that incorporating background knowledge during training can help improve the performance of the models, particularly when the Gödel t-norm is used in the loss. The highest gains are at the level of location detection task, where we see improvements of over 1% f-mAP on the test set for both I3D and SlowFast. However, the action detection performance is also slightly improved, i.e. by 0.62% f-mAP in the SlowFast case.

**Added Requirements**


---

```

{Ped, not Xing, Cyc, SmalVeh}
{Ped, not Wait2X, Cyc, SmalVeh}
{Ped, not Stop, Car, Cyc, Mobike, MedVeh, LarVeh, Bus, EmVeh, SmalVeh}
{Ped, not Mov, Car, Cyc, Mobike, MedVeh, LarVeh, Bus, EmVeh, SmalVeh}
{Ped, not MovTow, Car, Cyc, Mobike, MedVeh, LarVeh, Bus, EmVeh, SmalVeh}
{Ped, not MovAway, Car, Cyc, Mobike, MedVeh, LarVeh, Bus, EmVeh, SmalVeh}
{Ovtak, not EmVeh, MovAway, MovTow, Mov, Brake, Stop, IncatLft, IncatRht, HazLit, TurLft, TurRht, MovLft, MovRht, XingFmLft,
  XingFmRht, Rev}
{Ovtak, not Bus, MovAway, MovTow, Mov, Brake, Stop, IncatLft, IncatRht, HazLit, TurLft, TurRht, MovLft, MovRht, XingFmLft,
  XingFmRht, Rev}
{Ovtak, not LarVeh, MovAway, MovTow, Mov, Brake, Stop, IncatLft, IncatRht, HazLit, TurLft, TurRht, MovLft, MovRht, XingFmLft,
  XingFmRht, Rev}
{Ovtak, not Mobike, MovAway, MovTow, Mov, Brake, Stop, IncatLft, IncatRht, HazLit, TurLft, TurRht, MovLft, MovRht, XingFmLft,
  XingFmRht, Rev}
{Xing, not Cyc, MovAway, MovTow, Mov, Brake, Stop, IncatLft, IncatRht, TurLft, TurRht, Ovtak, Wait2X, XingFmLft, XingFmRht,
  Rev, MovLft, MovRht}
{Xing, not SmalVeh, MovAway, MovTow, Mov, Brake, Stop, IncatLft, IncatRht, TurLft, TurRht, Ovtak, Wait2X, XingFmLft, XingFmRht,
  Rev, MovLft, MovRht}
{Ovtak, not MedVeh, MovAway, MovTow, Mov, Brake, Stop, IncatLft, IncatRht, HazLit, TurLft, TurRht, MovLft, MovRht, XingFmLft,
  XingFmRht, Rev}
{Ovtak, not Car, MovAway, MovTow, Mov, Brake, Stop, IncatLft, IncatRht, HazLit, TurLft, TurRht, MovLft, MovRht, XingFmLft,
  XingFmRht, Rev}
{VehLane, OutgoLane, OutgoCycLane, IncomLane, IncomCycLane, Pav, LftPav, RhtPav, Jun, xing, BusStop, parking, rightParking,
  {not MovRht, not MovLft}}
{PushObj, not Ped, MovAway, MovTow, Mov, Stop, TurLft, TurRht, Wait2X, XingFmLft, XingFmRht, Xing}
{not Car, not SmalVeh}
{not Cyc, not SmalVeh}
{not Mobike, not SmalVeh}
{not MedVeh, not SmalVeh}
{not LarVeh, not SmalVeh}
{not TL, not SmalVeh}
{Ped, Car, Cyc, Mobike, MedVeh, LarVeh, Bus, EmVeh, TL, SmalVeh}
{not SmalVeh, not Green}
{not SmalVeh, not Red}
{not SmalVeh, not Amber}
LftParking, IncomBusLane, OutgoBusLane, TL}
{not rightParking, not LftParking}
{not rightParking, not VehLane}
{not rightParking, not OutgoLane}
{not rightParking, not OutgoCycLane}
{not rightParking, not IncomLane}
{not rightParking, not IncomCycLane}
{not rightParking, not Pav}
{not rightParking, not LftPav}
{not rightParking, not RhtPav}
{not rightParking, not Jun}
{not rightParking, not Xing}
{not rightParking, not BusStop}
{not rightParking, not parking}
{not LftParking, not VehLane}
{not LftParking, not OutgoLane}
{not LftParking, not OutgoCycLane}
{not LftParking, not IncomLane}
{not LftParking, not IncomCycLane}
{not LftParking, not Pav}
{not LftParking, not LftPav}
{not LftParking, not RhtPav}
{not LftParking, not Jun}
{not LftParking, not Xing}
{not LftParking, not BusStop}
{not LftParking, not parking}
{not OutgoBusLane, not IncomBusLane}
{not Stop, not Rev}
{not TL, not Rev}

```

---

**Table 9:** Set of requirements added to the ROAD-R set.



---

**Removed Requirements**

{PushObj, not Ped, MovAway, MovTow, Mov, Stop, TurLft, TurRht, Wait2X, XingFmLft, XingFmRht, Xing}  
 {Ped, not XingFmRht, Car, Cyc, Mobike, MedVeh, LarVeh, Bus, EmVeh}  
 {Ped, not XingFmLft, Car, Cyc, Mobike, MedVeh, LarVeh, Bus, EmVeh}  
 {Ped, not Wait2X, Cyc}  
 {Ped, not Stop, Car, Cyc, Mobike, MedVeh, LarVeh, Bus, EmVeh}  
 {Ped, not Mov, Car, Cyc, Mobike, MedVeh, LarVeh, Bus, EmVeh}  
 {Ped, not MovTow, Car, Cyc, Mobike, MedVeh, LarVeh, Bus, EmVeh}  
 {Ped, not MovAway, Car, Cyc, Mobike, MedVeh, LarVeh, Bus, EmVeh}  
 {Ovtak, not EmVeh, MovAway, MovTow, Mov, Brake, Stop, IncatLft, IncatRht, HazLit, TurLft, TurRht, XingFmRht, XingFmLft, Xing}  
 {Ovtak, not Bus, MovAway, MovTow, Mov, Brake, Stop, IncatLft, IncatRht, HazLit, TurLft, TurRht, XingFmRht, XingFmLft, Xing}  
 {Ovtak, not LarVeh, MovAway, MovTow, Mov, Brake, Stop, IncatLft, IncatRht, HazLit, TurLft, TurRht, XingFmRht, XingFmLft, Xing}  
 {OthTL, not Green, TL}  
 {OthTL, not Amber, TL}  
 {OthTL, not Red, TL}  
 {Ovtak, not Mobike, MovAway, MovTow, Mov, Brake, Stop, IncatLft, IncatRht, HazLit, TurLft, TurRht, XingFmRht, XingFmLft, Xing}  
 {Xing, not Cyc, MovAway, MovTow, Mov, Brake, Stop, IncatLft, IncatRht, TurLft, TurRht, Ovtak, Wait2X, XingFmLft, XingFmRht}  
 {Ovtak, not Car, MovAway, MovTow, Mov, Brake, Stop, IncatLft, IncatRht, HazLit, TurLft, TurRht, XingFmRht, XingFmLft, Xing}  
 {not Car, not OthTL}  
 {not Cyc, not OthTL}  
 {not Mobike, not OthTL}  
 {not Brake, not Cyc}  
 {not MedVeh, not OthTL}  
 {Ped, Car, Cyc, Mobike, MedVeh, LarVeh, Bus, EmVeh, TL, OthTL}  
 {not LarVeh, not OthTL}  
 {not Bus, not OthTL}  
 {not EmVeh, not OthTL}  
 {not TL, not OthTL}  
 {Ped, Cyc, not Xing}  
 {not OthTL, not MovAway}  
 {not MovTow, not OthTL}  
 {not OthTL, not Mov}  
 {not OthTL, not Brake}  
 {not Stop, not OthTL}  
 {not OthTL, not IncatLft}  
 {not OthTL, not IncatRht}  
 {not OthTL, not HazLit}  
 {not OthTL, not TurLft}  
 {not TurRht, not OthTL}  
 {not OthTL, not Ovtak}  
 {not OthTL, not Wait2X}  
 {not OthTL, not XingFmLft}  
 {not OthTL, not XingFmRht}  
 {not OthTL, not Xing}  
 {not OthTL, not PushObj}  
 {not OthTL, not Ped}  
 {VehLane, OutgoLane, OutgoCycLane, IncomLane, IncomCycLane, Pav, LftPav, RhtPav, Jun, XingLoc, BusStop, parking, TL, OthTL}  
 {Ovtak, not MedVeh, IncomLane, MovAway, MovTow, Mov, Brake, Stop, IncatLft, IncatRht, HazLit, TurLft, TurRht, XingFmLft, XingFmRht}

---

**Table 10:** Set of requirements removed from the ROAD-R set.

**Table 11:** Number of video- and frame-level instances for each individual label on the left. Corresponding frame-/video-level results (mAP@%) for the Test set. The results presented here are generated with the I3D backbone.

Classes	#All instances #Boxes/#Tubes	#Test instances #Boxes/#Tubes	Test
<b>Agent results</b>			
Car	2768704/35303	571655/7072	33.3/9.5
Ped	867407/11759	154767/2186	22.9/1.7
MedVeh	304636/3239	66114/692	18.5/15.1
TL	75031/762	17309/173	53.5/4.5
LarVeh	50382/477	10493/98	4.2/3.0
Bus	42167/362	8263/72	11.7/4.9
Cyc	18510/241	6616/80	0.9/0.1
Mobike	10186/146	2184/38	0.5/0.0
EmVeh	3535/37	1396/11	0.2/0.1
SmalVeh	3119/36	364/5	0.1/0.0
Ztotal	4143677/52362	839161/10427	14.6/3.9
<b>Action results</b>			
Stop	2234275/26405	467165/5605	31.5/9.3
MovAway	745421/7681	132165/1412	24.7/9.2
MovTow	586650/9635	92598/1607	16.7/6.1
Brake	241569/2039	53118/458	32.8/15.9
Mov	93894/1759	12699/348	1.5/0.1
XingFmRht	90751/2122	15160/436	11.9/3.1
XingFmLft	86992/2206	14597/507	15.0/4.7
Wait2X	63043/613	8115/121	2.8/0.7
Xing	46580/677	4921/62	12.4/1.6
Red	46340/331	9617/77	42.9/3.2
IncatLft	37787/461	9618/110	7.3/5.8
TurRht	28661/577	6682/129	2.8/0.9
IncatRht	27639/327	6692/83	2.1/1.9
Green	26271/393	7013/86	55.6/4.8
TurLft	25144/473	5578/101	7.8/6.9
HazLit	23786/184	4965/39	5.5/2.3
MovLft	9343/158	2087/32	0.9/1.0
MovRht	8608/146	1737/30	1.5/0.9
PushObj	6696/96	1374/26	0.3/0.1
Amber	1461/25	523/8	0.2/0.0
Ztotal	4433378/56329	856656/11279	12.5/3.6
<b>Location results</b>			
RightParking	767788/9133	157356/1937	34.6/9.6
LftParking	755289/8968	180327/2021	29.8/8.2
Jun	686943/10589	133504/2216	19.5/6.4
OutgoLane	575209/5175	102847/889	28.2/13.7
IncomLane	532911/8147	89862/1251	25.3/8.6
RhtPav	286766/4051	37954/829	8.9/0.7
VehLane	253559/1938	54418/386	26.9/12.7
LftPav	229461/3327	21146/523	5.1/0.1
Pav	85781/1713	15396/449	1.3/0.0
Parking	78769/1323	18172/275	1.8/1.3
Xing	17468/236	1259/20	0.5/0.0
BusStop	13035/174	2964/33	0.7/0.0
OutgobusLane	4237/32	321/1	0.9/0.0
IncombusLane	4113/34	809/7	3.2/3.2
OutgoCycLane	2444/22	770/6	2.3/16.7
IncomCycLane	2387/30	477/6	0.0/0.0
Ztotal	4296160/54892	817582/10849	11.8/5.1

**Table 12:** Number of video- and frame-level instances for the duplex label on the left. Corresponding frame-/video-level results (mAP@%) for the Test set. The results presented here are generated with the I3D backbone.

Classes	#All instances #Boxes/#Tubes	#Test instances #Boxes/#Tubes	Test
<b>Duplex results</b>			
Car-stop	1746379/20414	382924/4387	29.7/9.4
Car-movaway	504671/4830	92966/844	26.7/12.0
Car-movtow	374662/6673	64671/1045	17.6/7.3
Ped-stop	214349/3368	23447/641	2.1/0.0
Car-brake	209903/1803	48146/415	31.9/16.1
Medveh-stop	205892/2017	45568/444	15.8/15.9
Ped-movaway	172274/2331	25452/461	4.7/0.6
Ped-movtow	154347/2162	15812/403	3.5/0.2
Ped-mov	86786/1604	12069/334	1.5/0.1
Ped-wait2x	53768/516	7062/106	3.1/0.7
Ped-xing	46401/675	4829/60	13.5/1.9
Tl-red	46299/330	9576/76	43.8/4.3
Medveh-movaway	43739/333	8729/60	11.7/22.7
Ped-xingfmrht	41432/571	3323/81	10.2/1.1
Car-xingfmrht	41065/1365	9987/318	13.6/5.3
Ped-xingfmlft	39393/531	3922/88	17.4/4.3
Car-xingfmlft	38337/1444	8132/355	13.8/5.3
Medveh-movtow	37377/558	7449/104	6.2/11.1
Car-incatlft	31390/397	8057/95	6.9/4.3
Larveh-stop	30080/251	6507/47	6.2/4.6
Tl-green	26271/393	7013/86	55.7/8.2
Car-turrht	24367/503	5185/104	1.8/0.5
Car-incatrht	23515/281	5643/72	1.8/1.7
Medveh-brake	22677/177	3818/36	9.9/11.2
Car-turlft	21576/424	4769/85	6.8/4.3
Bus-stop	21425/157	4555/32	5.2/4.6
Larveh-movaway	9614/67	1477/13	0.2/1.1
Mobike-stop	9143/129	1994/34	0.5/0.1
Car-hazlit	9041/77	1535/14	0.3/0.0
Car-movlft	8008/139	1958/30	1.2/1.3
Bus-movaway	7972/61	1113/9	7.9/13.7
Car-movrht	7786/136	1441/28	0.9/0.5
Larveh-movtow	7313/99	1341/18	0.6/0.1
Ped-pushobj	6696/96	1374/26	0.3/0.1
Bus-movtow	6264/60	986/11	5.2/11.3
Cyc-movaway	6226/60	2235/23	2.9/4.3
Bus-brake	5678/41	740/6	14.0/3.3
Medveh-hazlit	5619/41	1266/11	1.1/0.0
Cyc-movtow	5454/71	2221/24	0.2/0.0
Medveh-xingfmlft	5099/142	1227/34	2.8/2.7
Bus-hazlit	4627/34	1146/8	7.5/6.0
Medveh-xingfmrht	4625/118	1148/24	3.0/1.2
Medveh-incatlft	4512/45	1147/11	0.9/3.8
Larveh-hazlit	4355/31	874/5	1.1/0.1
Medveh-incatrht	2897/30	962/9	0.8/0.0
Medveh-turrht	2676/49	1028/19	4.1/2.1
Emveh-stop	2400/21	1331/10	0.1/0.0
Cyc-stop	2186/25	627/7	0.0/0.0
Tl-amber	1461/25	523/8	0.4/0.0
Ztotal	4388027/55705	849305/11161	8.5/4.3

**Table 13:** Number of video- and frame-level instances for the triplet (event) label on the left. Corresponding frame-/video-level results (mAP@%) for the Test set. The results presented here are generated with the I3D backbone.

Classes	#All instances #Boxes/#Tubes	#Test instances #Boxes/#Tubes	Test
<b>Duplex results</b>			
Car-movaway-outgolane	363453/3524	61027/558	21.0/10.8
Car-movtow-incomlane	344150/6244	57577/943	18.8/7.5
Car-stop-jun	207234/1054	47875/448	9.1/4.3
Car-movaway-vehlane	131092/1017	29618/222	21.6/9.6
Car-brake-outgolane	127113/1135	28606/257	21.1/12.5
Car-stop-outgolane	121753/1093	25169/211	17.3/9.9
Car-stop-incomlane	112897/941	18495/145	9.8/2.3
Ped-movaway-rhtpav	100731/1313	17761/295	4.5/0.7
Ped-stop-rhtpav	85773/1263	9594/240	2.0/0.0
Car-brake-jun	79936/683	17514/153	13.0/5.8
Ped-stop-lftpav	79075/1218	6474/196	1.5/0.0
Ped-movtow-rhtpav	77477/1104	8011/225	3.3/0.2
Car-movaway-jun	69765/982	12171/174	7.2/5.5
Car-brake-vehlane	69674/509	16464/108	27.6/16.6
Ped-movtow-lftpav	69633/964	6850/156	2.9/0.3
Car-stop-parking	68115/1227	15812/259	1.3/1.0
Ped-movaway-lftpav	63763/906	6561/147	1.1/0.0
Car-stop-vehlane	63405/484	15168/102	21.5/11.5
Car-movtow-jun	55820/1042	9640/184	3.1/2.5
Ped-mov-pav	53225/1050	9602/273	1.8/0.1
Ped-wait2x-jun	43077/419	5791/76	2.0/0.1
Car-xingfnrht-jun	40841/1358	9968/317	13.3/4.9
Ped-xingfnrht-jun	38525/528	2282/68	11.7/1.2
Car-xingfnlft-jun	38150/1440	8108/353	13.5/5.8
Ped-xingfnlft-jun	35941/493	3649/81	17.9/4.7
Ped-xing-jun	35067/510	4793/58	12.7/1.5
Medveh-movtow-incomlane	33629/521	6201/91	7.3/9.3
Medveh-movaway-outgolane	32209/251	6625/43	11.4/21.1
Ped-stop-pav	25195/550	4278/152	0.1/0.0
Medveh-stop-jun	22801/187	5139/43	1.9/2.2
Car-turrht-jun	20987/421	4454/88	1.6/0.3
Car-turrlft-jun	18856/363	4064/69	7.0/2.9
Car-incatlft-jun	16397/225	4175/54	3.7/1.6
Medveh-stop-outgolane	16120/125	2769/21	1.7/1.7
Ped-mov-rhtpav	14476/283	685/33	0.1/0.0
Medveh-brake-outgolane	13012/111	2245/20	8.4/6.4
Medveh-stop-incomlane	12400/88	2681/17	1.2/2.5
Car-incatlft-incomlane	11298/128	3207/31	6.0/6.3
Car-incatrht-jun	11027/155	2420/40	0.9/0.1
Medveh-movaway-vehlane	10901/65	2054/14	2.7/10.4
Ped-stop-busstop	10814/152	2255/28	0.7/0.0
Car-incatrht-outgolane	9775/119	2299/28	0.8/1.5
Medveh-stop-vehlane	8163/53	1295/10	3.7/3.0
Medveh-brake-vehlane	7807/51	1128/9	5.3/3.0
Bus-stop-jun	7801/51	2141/11	2.0/1.5
Car-incatlft-outgolane	7332/103	1650/20	1.0/0.5
Medveh-brake-jun	7201/58	1340/15	2.7/2.6
Larveh-movtow-incomlane	6714/91	1229/15	0.9/0.4
Medveh-stop-parking	6697/99	1507/20	2.3/2.2
Car-incatlft-vehlane	5941/66	1484/18	4.9/1.0
Medveh-movtow-jun	5708/86	1472/21	1.4/8.6
Ped-wait2x-rhtpav	5494/58	511/19	0.6/0.7
Car-incatrht-vehlane	5373/61	1220/12	0.6/8.7
Car-movrht-outgolane	5362/81	1094/20	0.7/0.2
Medveh-xingfnlft-jun	5099/142	1227/34	2.3/1.9
Medveh-movaway-jun	5059/63	755/13	1.2/2.3
Medveh-xingfnrht-jun	4596/117	1148/24	2.4/0.8
Car-movlft-outgolane	4517/84	882/15	0.6/0.2
Bus-movtow-incomlane	4161/39	634/5	3.6/0.8
Larveh-movaway-vehlane	3953/23	966/6	0.4/0.5
Ped-stop-outgolane	3909/53	669/12	0.0/0.0
Larveh-stop-jun	3766/31	1232/8	0.0/0.0
Bus-stop-outgolane	3524/23	1053/7	6.9/4.6
Bus-stop-vehlane	2925/18	813/5	0.4/2.5
Bus-movaway-outgolane	2906/26	549/6	2.1/4.2
Car-incatrht-incomlane	2736/33	533/6	0.2/0.4
Ped-xingfnrht-xing	2708/40	945/13	0.4/0.0
Medveh-turrht-jun	2491/44	917/18	3.0/0.7
Larveh-stop-vehlane	2335/18	691/3	0.2/0.0
Ped-pushobj-rhtpav	2318/34	601/13	0.1/0.0
Car-turrlft-vehlane	2309/50	520/12	0.2/0.0
Bus-stop-incomlane	2298/19	820/6	0.0/0.0
Car-movlft-vehlane	2235/31	778/9	0.5/0.0
Cyc-movaway-outgocyclane	2071/17	714/5	1.9/20.0
Cyc-movtow-incomlane	2009/23	732/6	0.0/0.0
Car-movtow-vehlane	1886/13	632/4	0.1/0.0
Ped-pushobj-lftpav	1844/23	532/6	0.1/0.0
Ped-movaway-jun	1806/21	661/7	1.2/0.0
Car-hazlit-incomlane	1489/14	759/6	0.1/0.0
Ped-mov-outgolane	1436/18	587/8	0.0/0.0
Cyc-movaway-rhtpav	1430/14	620/7	0.0/0.0
Medveh-incatrht-jun	1423/17	516/8	0.5/0.0
Bus-hazlit-outgolane	1250/12	592/4	4.6/9.8
Medveh-incatlft-incomlane	1198/17	507/5	0.3/0.0
Ped-movtow-jun	1160/23	527/13	0.1/0.0
Cyc-movtow-rhtpav	907/12	846/10	0.0/0.0
Ztotal	3019199/39115	550160/7515	4.6/3.1

**Table 14:** Baseline *vs.* t-norm-based loss models, using SlowFast. Frame-level (mAP %) are calculated on ROAD-Waymo validation/test sets.

Model	Agents	Actions	Locations
SlowFast	16.01/ <b>17.90</b>	12.62/13.97	12.56/13.07
+ Gödel	<b>16.83</b> /17.85	<b>13.40</b> / <b>14.59</b>	<b>14.10</b> / <b>14.07</b>
+ Łukasiewicz	15.35/17.15	12.62/13.94	12.33/12.69